JOURNAL OF THE KOREAN ASTRONOMICAL SOCIETY
35: 29 ~ 34, 2002

UBVI CCD PHOTOMETRY OF THE OPEN CLUSTER NGC 559

HONG BAE ANN AND SANG HYUN LEE
Division of Science Education, Pusan National University, Pusan 609-735, Korea
E-mail: hbann@cosmos.es.pusan.ac.kr, shlee@jupiter.es.pusan.ac.kr
(Received Feb. 7, 2002; Accepted Mar. 12, 2002)

ABSTRACT

We have conducted *UBVI* CCD photometry of an intermediate-age open cluster NGC 559 to investigate the effect of dynamical evolution on the stellar distributions in NGC 559. Our photometry allows better estimates of distance and age of the cluster owing to much deeper photometry ($V \leq 21$) than previous ones. It is found that the luminosity function and mass function as well as the spatial stellar distributions are affected by the dynamical evolution. Mass segregation leads to the central concentration of the high mass stars, which results in the flattened mass function inside the half mass radius.

Key words : open clusters: individual (NGC 559) – distance – age – mass function – dynamical evolution

I. INTRODUCTION

Dynamical evolution of old and intermediate-age open clusters has been a main subject of open cluster study in recent years (de La Fuente 1997; Nordstroem, Andersen & Andersen 1997; Raboud & Mermilliod 1998a, b). The present day luminosity function (LF) and mass function (MF) as well as the stellar density distribution are much different from the initial ones. Stellar evolution plays a key role in the evolution of the stellar content of open clusters and the effect of dynamical evolution on the LF and MF is thought to be significant. High mass stars are likely to be found in the central part of the cluster due to mass segregation, while low mass stars are likely to move outward and some of them escape from the cluster eventually. Because the membership of cluster stars is critical for the investigation of the dynamical properties of clusters, most of the previous studies are focused on the nearby clusters whose member stars are easily discernible from field stars (Pels, Oort, & Pels-Kluyver 1975; Raboud & Mermilliod 1998a, b) or on the rich clusters whose dynamical properties can be analyzed statistically (Sung et al. 1999; Lee, Kang & Ann 1999; Kang 2000). However, more than half of the known open clusters are known to have a small number of member stars which are difficult to be isolated from the field stars (e.g., Ann et al. 1999, 2002).

NGC 559 is located in the direction of ($l = 127.^\circ2, b = 0.^\circ75$). As indicated by its Trumpler class of $I1m$, it is a centrally concentrated cluster with a medium number of member stars. The distance and reddening of the cluster have been determined by photoelectric (Lindoff 1969; Jennens & Helfer 1975) and photographic (Grubissich 1975) photometries but there are a large discrepancies in the derived parameters, especially for the distance. Lindoff (1969) determined a distance modulus of $(m - M)_0 = 10.6$, while Jennens & Helfer (1975) derived $(m - M)_0 = 14.0$. The distance estimate of Grubissich (1975) is similar to that of Lindoff (1969) but his *RGU* photometry was calibrated from the Lindoff (1969)'s photometry. There is also some discrepancy in the age estimates of NGC 559. Lindoff (1969) considered that NGC 559 has an age of $\sim 10^9$ yr but Jennens & Helfer (1975) thought that it is a relatively young cluster of $\sim 10^8$ yr. However, we expect that NGC 559 is a dynamically relaxed cluster since it's age inferred from the CMD morphology seems to be much larger than the supposed dynamical relaxation time of the cluster.

The purpose of the present study is to investigate the dynamical properties of NGC 559, by conducting a deep *UBVI* CCD photometry, along with accurate estimates of the cluster physical parameters. In Section II, we describe the observations and data reductions, and the cluster parameters are derived in Section III. We describe the photometric memberships in Section IV and the dynamical properties are analyzed in Section V. The summary and discussion are given in the last section.

II. OBSERVATIONS AND DATA REDUCTION

(a) Observations

The observations in *UBVI* pass bands were carried out for a field of NGC 559 on two nights of October 1998, with Photometrics 512 × 512 CCD which was attached to the cassegrain focus of the 61cm telescope at the Sobaeksan Astronomical Observatory (SOAO). Additional observations of NGC 559 were made in *VI* pass bands with SITe 2048 × 2048 CCD attached to

Corresponding Author: H. B. Ann

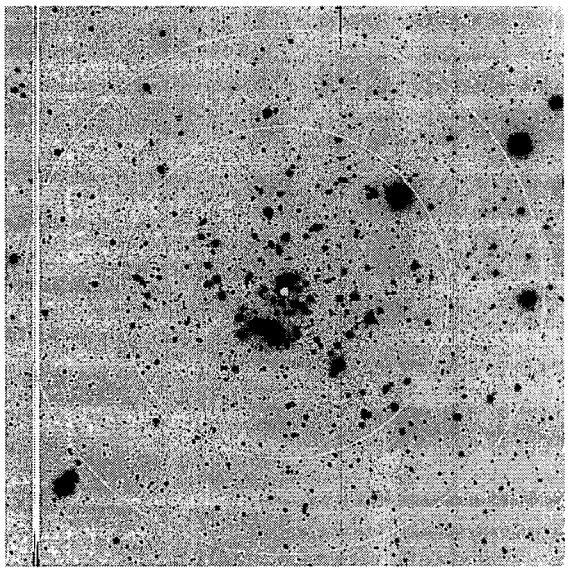

Fig. 1.— Greyscale maps of the V-band CCD image of NGC 559. The center of the cluster is indicated by a white dot. The inner circle represents the half mass radius and the outer circle represents the cluster boundary beyond which stars are considered to be field stars. North is up and East is to the left.

the 1.8m telescope of Bohyunsan Astronomical Observatory (BOAO) on a night of February 1999. The pixel size of the 512 × 512 CCD and the 2048 × 2048 CCD are 0.″5 and 0.″34, respectively.

We observed a region of 11.′5 × 11.′5, centered on NGC 559, which is mosaicked by 3 × 3 Photometrics CCD frames. For field star corrections, we observed additional four regions which are ∼ 40′ apart from the cluster center and located in the south-east, north-east, south-west, and north-west of the cluster. The BOAO observations covered 11.′8 × 11.′8 region centered on the cluster. The seeing of SOAO images is about 1″ and that of BOAO images is about 2″. Fig. 1 shows the BOAO V-band image of NGC 559. Bias and dark frames were obtained several times during the nights and the flat-field exposures were made on the twilight sky. For the calibration purposes, several standard stars in SA98 and SA110 regions (Landolt 1992) as well as NGC 7790 (Sandage 1955; Christian et al. 1985) were observed in V and I bands in the October run. The journal of the observations is given in Table 1.

Table 1. Observational log of NGC 559

Filter	T_{exp}(SOAO)	T_{exp}(BOAO)
U	300s × 20	
B	300s × 9	
V	120s × 3	300s, 25s
I	60s × 3	70s, 7s

(b) Reduction

The basic CCD reduction was carried out using the CCDRED package within IRAF. This procedure involved the subtraction of the mean bias frame with overscan correction, trimming of the data section, and flat-fielding. We do not correct the dark current because it is negligible in both of the observing runs. We applied PSF photometry to obtain instrumental magnitudes using IRAF/DAOPHOT. The transformation of the instrumental magnitudes of SOAO observations to the standard system were made by the following equations,

$$U = u - 7.878 + 0.196(U - B)$$
$$B = b - 6.006 + 0.120(B - V)$$
$$V = v - 4.808 - 0.003(V - I) - 0.341X$$
$$I = i - 5.203 + 0.023(V - I) - 0.189X$$

where the capital letters stand for the magnitudes in the standard system, the lower case letters for the instrumental magnitudes, and X for the airmass. The coefficients in the transformation equations of V and I bands were derived from the standard star observations at SOAO while those of B and U bands were derived from the photoelectric photometries of Jennens & Helfer (1975), Lindoff (1969) and Cardon (1982). Fig. 2 shows the residuals of the calibration of the present photometry, showing that the standard deviations of the calibration are ∼ 0.03 mag in B, V, and I and ∼ 0.08 mag in U, respectively

The transformation of the instrumental magnitudes of BOAO observations were made by the following equations derived from the magnitudes of the local standard stars from the SOAO observations,

$$V = v - 2.518 - 0.017(V - I)$$
$$I = i - 2.282 + 0.036(V - I)$$

where the capital letters stand for the magnitudes in the standard system and the lower case letters for the instrumental magnitudes.

III. PHYSICAL PARAMETERS

The distance, reddening, age and metallicity of NGC 559 have been determined from the previous photoelectric and photographic photometries (Lindoff 1969; Jennens & Helfer 1975; Grubissich 1975). But the previous estimates of the physical parameters are supposed to be less accurate because their photometries were confined to stars brighter than $V \sim 15$. Thus, we have determined the distance, reddening, age and metallicity of NGC 559 using the present photometry of SOAO observations.

The reddening toward NGC 559 was determined by fitting the fiducial ZAMS (Schmidt-Kaler 1982) to the stellar distributions in the $U - B$ vs $B - V$ diagram,

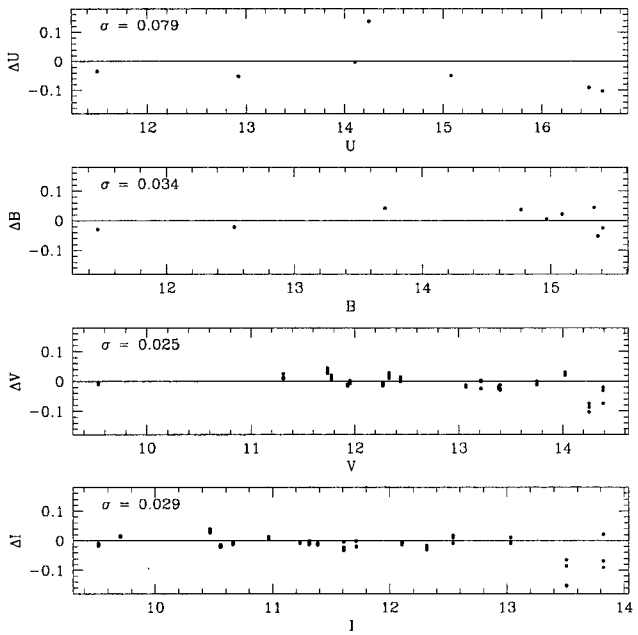

Fig. 2.— Residuals (standard magnitudes minus transformed magnitudes) of the standard transformation for U, B, V and I.

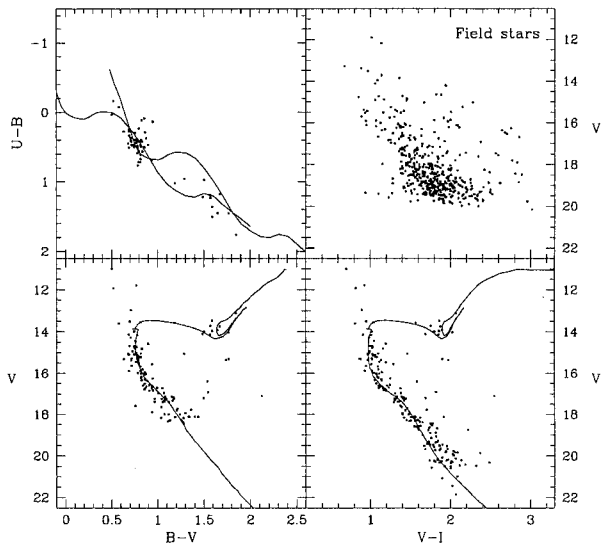

Fig. 3.— Color-color diagram and CMDs of NGC 559. The solid line in the color-color diagram represents the ZAMS, and the lines in the CMDs represent the Padova theoretical isochrones with log(t[yr]) = 8.6 and [Fe/H] = −0.32 dex, shifted according to the reddening ($E(B-V) = 0.81$) and distance ($(m-M)_0 = 11.8$) of NGC 559.

while the distance, age and metallicity of the cluster were determined simultaneously by isochrone fittings to the stellar distributions in the V vs $V-I$ CMD. We used the Padova isochrones (Bertelli et al. 1994) and assumed $E(U-B)/E(B-V) = 0.72$ (Johnson & Morgan 1953), $E(V-I) = 1.25E(B-V)$ (Dean, Warren, & Cousins 1978) and a total to selective extinction ratio of R_V=3.0. In general, metallicity is virtually a free parameter in isochrone fittings. However, in case of NGC 559, it is not a completely free parameter in isochrone fittings because it can be constrained by the locations of the giant stars in the CMD.

Our reddening estimate of $E(B-V) = 0.81 \pm 0.05$ is somewhat larger than the previous estimates of $E(B-V) = 0.54$ (Lyngå1987) and $E(B-V) = 0.62$ (Jennens & Helfer 1975). The reason for the large discrepancies is mainly due to the exclusion of three bright stars near $B-V \approx 0.5$ in the present ZAMS fitting, while they were included in the previous estimates. However, due to the large photometric errors of the present photometry in U, it is difficult to derive accurate $E(B-V)$ from the present photometry.

Fig. 3 shows the resulting best fit isochrone which gives the cluster parameters as $(m-M)_0 = 11.8 \pm 0.2$, log(t[yr]) = 8.6 ± 0.1 and [Fe/H] = −0.32 dex with $E(B-V) = 0.81 \pm 0.05$. We list the present estimates of the physical parameters with those of the previous studies in Table 2. As shown in Table 2, the present estimates of the age of NGC 559 is in a good agreement with those of previous studies but the present estimate of the reddening and metallicity are somewhat larger than the previous ones.

IV. PHOTOMETRIC MEMBERSHIP

The membership of cluster stars is crucial to analyze the dynamical properties of open clusters. Conventional method of membership determination of open clusters is to use the kinematical properties of cluster stars. However, most of the proper motion studies do not reach the lower main-sequencer stars and the observations of radial velocities have been confined to bright stars until recently. For NGC 559, the proper motion study of de Graeve (1979) are confined to stars brighter than $V \sim 16$. Thus, we employ a photometric membership to analyze the dynamical properties of NGC 559.

Fig. 4 shows the V vs $V-I$ CMD of NGC 559 constructed from the BOAO observations. We do not use SOAO observations in the analysis of the dynamical properties because the limiting magnitude of SOAO observations is $\sim$ 2 mag brighter than that of BOAO observations. As shown in Fig. 4, we selected two regions in the CMD to define the photometric regions for

Table 2. Physical parameters of NGC 559

$(m-M)_0$	log(age)	[Fe/H]	$E(B-V)$	References
11.8 ± 0.2	8.6 ± 0.1	-0.32	0.81 ± 0.05	1
10.3	8.7	−0.76	0.54	2
14.0	7.7	−1.00	0.62	3
12.3	9.1			4, 5

1 This studt, 2 Lyngå(1987), 3 Jennens & Helfer (1975), 4 Grubissich (1975), 5 Lindoff (1968)

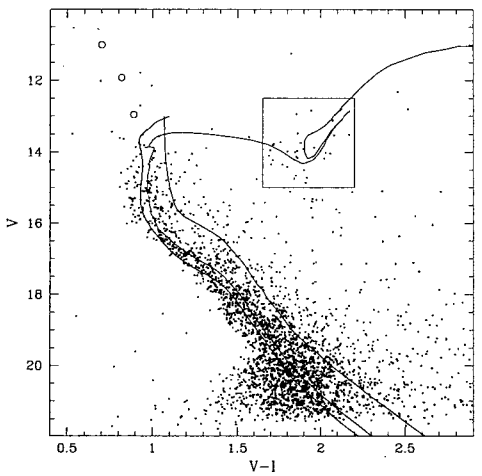

Fig. 4.— Photometric membership criteria for main sequence stars and giant stars. The lower and upper boundaries of the cluster main sequence are set by the cluster isochrone and the binary sequence, respectively, with the photometric errors of (0.15 ~ 0.3) mag. The three blue straggler candidates are plotted by open circles.

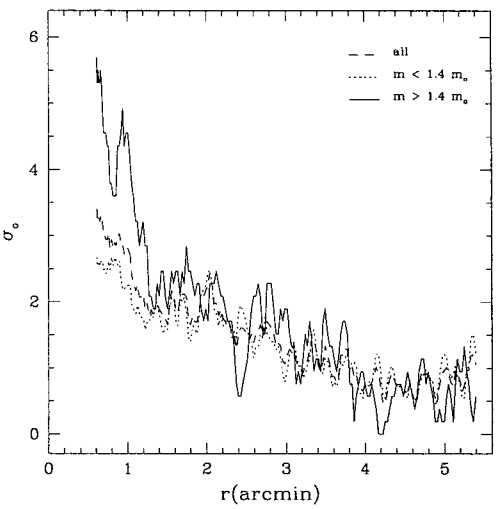

Fig. 5.— Radial surface number density distribution of stars with photometric membership probability greater than 0.5. The solid line represents the distribution of stars with $m > 1.4\,M_{\odot}$ and the dotted line indicates the stars with $m < 1.4\,M_{\odot}$, respectively. The distribution of all the stars with membership probability greater than 0.5 is designated by the dashed line.

the cluster stars. For main sequence stars, by considering the photometric errors of (0.15 ~ 0.3) mag, we set the fitted isochrone as the lower envelope and the equal-mass binary sequence, which lies 0.75mag above the ZAMS, as the upper envelope, respectively. But, we select a photometric box for the giant stars by considering the isochrone morphology in the giant branch region. If a star is found in one of the two regions in the CMD, we consider it as a probable cluster member. However, some of these stars are not real cluster members because field stars can be located in the photometric regions defined for the cluster members.

For stars in the cluster regions, the photometric membership probability of a star with a visual magnitude V can be defined by the ratio of the number of cluster member stars to the total number of stars in the magnitude range of $V - \Delta V \leq V < V + \Delta V$,

$$P = \frac{N_c}{N_t} \qquad (1)$$

where N_t is the total number of stars in a magnitude bin and N_c is the number of cluster stars in the same bin, respectively. To determine the number of cluster stars, it is necessary to know the number of field stars which are located in the photometric regions of the cluster stars. Because there was no separate observation of field region at the BOAO, we obtained the field star CMD from the stars outside the radius of 5.′45 from the BOAO CCD images. The number of field stars in the photometric region was scaled to the same area as that of the cluster region.

The open circles in Fig. 4 represent three blue straggler candidates that have high membership probabilities by proper motion study (de Gravae 1979). In the decreasing order of the brightness, their membership probabilities are 0.88, 0.84 and 0.92, respectively.

V. DYNAMICAL PROPERTIES

(a) Number Density Distribution

Fig. 5 shows the distribution of surface number density of stars that have photometric membership probability greater than 0.5. The surface density in Fig. 5 is a running mean average of surface density with a smoothing radius of 150 pixels. We divide the stars in two groups according to their masses derived from the cluster isochrone: $m > 1.4\,M_{\odot}$, $m < 1.4\,M_{\odot}$. There seems to be no big difference between the two groups in the outer part of the cluster and we can see that the cluster ends near $r \approx 4.'5$. However, there is an appreciable difference between the two groups in the central part of the cluster. The surface density of high mass stars is about two times higher than that of the low mass stars inside $r < 1'$. This is an evidence of dynamical evolution in NGC 559. High mass stars moved to the inner part of the cluster while low mass stars moved to the outer part due to mass segregation.

(b) Half Mass Radius

The angular diameter of a cluster is a poorly defined quantity which seems to have no direct relation-

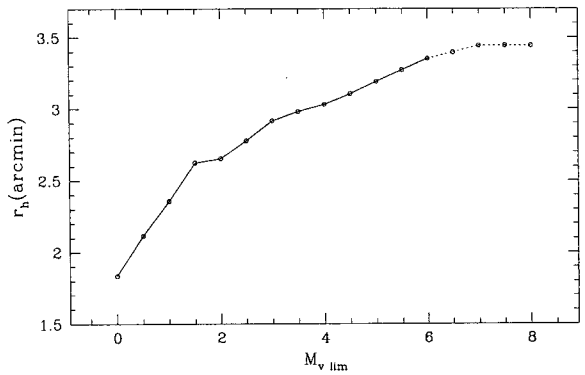

Fig. 6.— Half mass radius as a function of limiting magnitudes of photometry. The dotted lines represent the limiting magnitudes derived from the large photometric errors.

ship to its dynamical properties. A more meaningful quantity, which is related to the dynamical properties of a cluster, is the half mass radius r_h, defined by the radius within which the half of cluster mass is contained. By using stellar masses determined from the cluster isochrone and the photometric probabilities, we derived r_h from the equation,

$$\frac{\int_0^{r_h} \sum m_i(r) P_i(r) dr}{\int_0^{r_c} \sum m_i(r) P_i(r)} = \frac{1}{2} \qquad (2)$$

where m_i and P_i are mass and photometric membership probability of a star, respectively, and r_c is the cluster radius. We adopted r_c as 4.′5 from the stellar density distribution in Fig. 5. The resulting r_h of NGC 559 is 3.′4 and it is plotted as the small circle in Fig. 1. However, the true value of r_h is larger than the derived value of 3.′4 because, for a dynamically relaxed cluster, r_h depends on the limiting magnitudes of the observed images. Fig. 6 shows the variation of r_h as a function of radius. The gradual increase of r_h with increasing limiting magnitudes is caused by the mass segregation which leads to the concentration of massive stars in the central part of the cluster. Thus, it is evident that NGC 559 is dynamically well relaxed.

(c) Luminosity and Mass Function

The LF and MF of open clusters are known to vary with time due to dynamical evolution as well as stellar evolution. The high mass stars disappear due to stellar evolution while the low mass stars evaporate from the cluster due to dynamical evolution. Fig. 7 shows the LFs and MFs of NGC 559. The bottom panels represent the LF and MF of the entire field and the top and middle panels represent the LFs and MFs of the inner region ($r < r_h$) and the outer region ($r > r_h$), respectively.

As shown in the bottom left panel of Fig. 7, the LF of NGC 559 shows the typical characteristics of intermediate-age open clusters with a gap at $MV \sim$

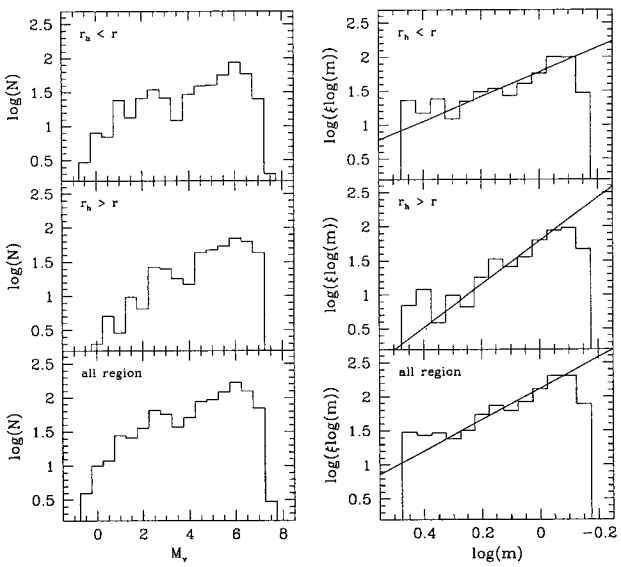

Fig. 7.— Luminosity functions and mass functions of NGC 559. They are corrected for field star contaminations.

3.5. Similar gaps, which are known as Böhm-Vitense gap, have been reported in several open clusters including Coma, Praesepe, and Hyades. They are interpreted as a result of the onset of surface convection zones in the stars with $B - V \approx 0.35$ (Böhm-Vitense, & Canterna 1974). Recent analysis of existing photometry of well surveyed 9 open clusters shows that 6 of 9 open clusters show the Böhm-Vitense gap near $B - V = 0.35$ (Rachford & Canterna 2000).

As shown in the top and middle panels of Fig. 7, there is a significant difference between the LFs and MFs of the inner and outer regions of NGC 559. There are more high mass stars in the inner region than the outer region, while there seems to be no pronounced difference in the low mass part of the LFs and MFs. Thus, the large difference in the slope of the MFs is mainly caused by the concentration of high mass stars in the central part of the cluster due to mass segregation. The slopes of the MFs of the inner region and the outer region are –1.81 and –3.17, respectively.

VI. SUMMARY AND DISCUSSION

We have derived the physical parameters of the open cluster NGC 559 by conducting a deep *UBVI* CCD photometry and isochrone fittings using Padova stellar evolution models (Bertelli et al. 1994). The distance of the cluster is found to be $\sim$ 2.3 kpc which is about three times smaller than that of Jennens & Helfer (1975) but slightly larger than that of Lindoff (1969). The age and metallicity of the cluster are estimated to be t $\approx 4 \times 10^8$ yr and [Fe/H] = –0.32, respectively.

The dynamical properties of NGC 559 were investigated by analyzing the stellar density distributions and luminosity and mass functions. The stellar num-

ber density distributions shows that high mass stars ($m > 1.4\,M_{\odot}$) are more centrally concentrated than the low mass ones ($m < 1.4\,M_{\odot}$). Because NGC 559 is old enough to be dynamically relaxed, the central concentration of high mass stars can be interpreted by the effect of mass segregation due to dynamical evolutions. The effect of mass segregation in NGC 559 is also indicated by the dependence of half mass radius r_h on the limiting magnitudes of the observations. The half mass radius becomes smaller as the limiting magnitude gets brighter.

The effect of dynamical evolution is also imprinted in the LFs and MFs of NGC 559. There are more number of high mass stars in the inner region ($r < r_h$) than in the outer region ($r > r_h$). Thus, derivation of initial mass functions from the MFs of open clusters should be cautious when the ages of the clusters are significantly older than the dynamical relaxation times.

This work was supported in part by grant No. R01-1999-00023 from the Korea Science & Engineering Foundation.

REFERENCES

Ann, H. B., et al. 1999, BOAO Photometric Survey of Galactic Open Clusters. I. Berkeley 14, Collinder 74, Biurakan 9, and NGC 2355, JKAS, 32, 7

Ann, H. B., et al. 2002, BOAO Photometric Survey of Galactic Open Clusters. II. Physical Parameters of 12 Open Clusters, AJ, 123, 905

Böhm-Vitense, E., & Canterna, R. 1974, The Gap in the Two-Color Diagram of Main-Sequence Stars, ApJ, 194, 629

Bertelli, G., Bressan, A., Chiosi, C., Fagotto, F., & Nasi, E. 1994, Theoretical isochrones from models with new radiative opacities, A&AS, 106, 275

Cardon de Lichtbuer, P. 1982, Photoelectric sequences for three open cluster: CO 126+630 (NGC 559), C2137+572 (TR 37) and and C 2152+623 (NGC 7160), Publ. Vatican Obs, 2, 1

Christian, C. A., Adams, M., Barnes, J. V., Hayes, D. S., Siegel, M., Butcher, H., & Mould, J. R. 1985, Video camera/CCD standard stars (KPNO video camera/CCD standards consortium), PASP, 97, 363

Dean, J. F., Warren, P. R., & Cousins, A. W. J. 1978, Reddenings of Cepheids using BVI photometry, 1978, MNRAS, 183, 569

de Graeve, E. 1979, Astrometric Criteria for Selecting Physical Members of Open Clusters with Low Astrometric Precision - Application to NGC559, Publ. Vatican Obs, 1, 283

de la Fuente Marcos, M. 1997, The initial mass function and the dynamical evolution of open clusters. IV. Realistic systems, A&A, 322, 764

Grubissich, C. 1975, Three-colour photometry of the two galactic star clusters NGC 559 and NGC 637, A&AS, 21, 99

Kang, Y.- W. 2000, Luminosity Function and Dynamical Evolution of Open Clusters, Ph.D. Thesis, Pusan National University

Jennens, P. A., & Helfer, H. L. 1975, Photometric metal abundances for twenty clusters, MNRAS, 172, 681

Johnson, H. L., & Morgan, W. W. 1953, Fundamental stellar photometry for standards of spectral type on the revised system of the Yerkes spectral atlas, ApJ, 117, 313

Landolt, A. U. 1992, UBVRI photometric standard stars in the magnitude range 11.5-16.0 around the celestial equator, AJ, 104, 340

Lee, S. H., Kang, Y. -W., & Ann, H. B. 1999, UBVI CCD Photometry of the Open Cluster NGC 2420, PKAS, 4, 61

Lindoff, V. 1969, The open cluster NGC 559, Arkiv astron, 5, 221

Lyngå, G. 1987, Lund Catalogue of Open Cluster Data (5th ed:ADC CD Rom Version)

Nordstroem, B., Andersen, J., & Andersen, M. I. 1997, Critical tests of stellar evolution in open clusters. II. Membership, duplicity, and stellar and dynamical evolution in NGC 3680, A&A, 322, 460

Pels, G., Oort, J. H., & Pels-Kluyver, H. A. 1975, New members of the Hyades cluster and a discussion of its structure, A&A, 43, 423

Raboud, D., & Mermilliod, J.-C. 1998, Investigation of the Pleiades cluster. IV. The radial structure, A&A, 329, 101

Raboud, D., & Mermilliod, J.-C. 1998, Evolution of mass segregation in open clusters: some observational evidences, A&A, 333, 897

Rachford, B. L., & Canterna, R. 2000, The Relationship Between the Böhm-Vitense Gap and Stellar Activity in Open Clusters, AJ, 119, 1296

Schmidt-Kaler, Th. 1982, in Landolt-Börnstein VI, 2b, Stars and Star clusters (Berlin: Springer-Verlag)

Sung, H., Bessell, M. S., Lee, H.-W., Kang, Y. H., & Lee, S.-W. 1999, UBVI CCD photometry of M11 - II. New photometry and surface density profiles, MNRAS, 310, 982